arXiv:2106.10654v1 [eess.AS] 20 Jun 2021

Encoder-Decoder Based Attractor Calculation for End-to-End Neural Diarization

Shota Horiguchi, *Member, IEEE,* Yusuke Fujita, *Member, IEEE,* Shinji Watanabe, *Senior Member, IEEE,* Yawen Xue, Paola García *Member, IEEE,*

***Abstract*—This paper investigates an end-to-end neural diarization (EEND) method for an unknown number of speakers. In contrast to the conventional pipeline approach to speaker diarization, EEND methods are better in terms of speaker overlap handling. However, EEND still has a disadvantage in that it cannot deal with a flexible number of speakers. To remedy this problem, we introduce encoder-decoder-based attractor calculation module (EDA) to EEND. Once frame-wise embeddings are obtained, EDA sequentially generates speaker-wise attractors on the basis of a sequence-to-sequence method using an LSTM encoder-decoder. The attractor generation continues until a stopping condition is satisfied; thus, the number of attractors can be flexible. Diarization results are then estimated as dot products of the attractors and embeddings. The embeddings from speaker overlaps result in larger dot product values with multiple attractors; thus, this method can deal with speaker overlaps. Because the maximum number of output speakers is still limited by the training set, we also propose an iterative inference method to remove this restriction. Further, we propose a method that aligns the estimated diarization results with the results of an external speech activity detector, which enables fair comparison against pipeline approaches. Extensive evaluations on simulated and real datasets show that EEND-EDA outperforms the conventional pipeline approach.**

***Index Terms*—Speaker diarization, EEND, EDA**

I. Introduction

SPEAKER diarization is a task of estimating multiple speakers' speech activities from input audio (sometimes referred to as the "who spoke when" problem). It can be placed as a downstream task of automatic speech recognition (ASR), in which speaker information is tagged to each transcribed utterance [1]–[3]. It can also be used as prior to speech separation and the following ASR. For example, in guided source separation [4], speech activities are used as constraints to update time-frequency masks of a complex angular central Gaussian mixture model. The speech-activity-driven speech-extraction neural network [5] takes acoustic features and a target speaker's speech activity to perform fully neural speech separation.

Classical pipeline methods treat speaker diarization as a partition problem. Given a set of time frames, they first detect speaker-active frames and then divide them into clusters by using speaker embeddings extracted with a sliding window. The number of clusters, which represents the number of speakers, is determined in the clustering step during inference. Eigen value analysis on the graph Laplacian of a similarity matrix calculated from frame-wise embeddings is one way to estimate the number of speakers explicitly [6], [7]. If agglomerative hierarchical clustering is employed as a clustering algorithm, a threshold value is usually preset, and the number of clusters, *i.e.*, the number of speakers, is dynamically determined by the threshold value [8]. Either way, the number of clusters can be set flexibly during inference. However, there is one fundamental problem that it basically cannot handle speaker overlaps because each speech frame is usually assigned to one speaker.

Some neural-network-based end-to-end methods, in comparison, naturally handle speaker overlap with a single network. For example, the Recurrent Selective Attention Network (RSAN) [9], [10] decodes speech activity for each speaker one by one until a stopping condition is satisfied. However, it requires clean speech to be trained as a mask-based speech separation model. End-to-end neural diarization (EEND) [11]–[13], which estimates multiple speakers' speech activities at once from input audio, does not require such clean speech for training. The limitation is that the original EEND fixes the output number of speakers; thus, knowing the number of speakers in advance is a requirement.

In our previous study [14], we introduced an encoder-decoder-based attractor calculation module (EDA) as part of the self-attentive EEND model [12] to handle unknown numbers of speakers (EEND-EDA). It calculates attractors from frame-wise embeddings using a sequence-to-sequence method with an LSTM encoder-decoder; thus, the number of attractors can be flexible. In general, sequence-to-sequence methods require a stopping criterion in their decoding process. To decide when to stop the attractor calculation, EDA also estimates whether each calculated attractor really corresponds to a speaker. The diarization results are calculated as dot products between the attractors and frame-wise embeddings. Despite being designed for the diarization of flexible numbers of speakers, it also has performed better than the original EEND under fixed-number-of-speakers conditions. Compared with other EEND extensions for unknown numbers of speakers [15], [16], it performed the best on various datasets including the CALLHOME and DIHARD III datasets [17].

In this paper, we revisit EEND-EDA with more comprehensive discussions and formulations and propose several extensions from the original EEND-EDA presented in [14]. We discuss the relationship between the original EEND and EEND-EDA, which explains EEND-EDA's better performance

S. Horiguchi and Y. Xue are with Hitachi, Ltd.
Y. Fujita is with LINE corporation. This work had been done during he was with Hitachi, Ltd.
S. Watanabe is with Carnegie Mellon University.
P. García is with Johns Hopkins University.

in a fixed-number-of-speakers evaluation. We also propose refining the training strategy of EEND-EDA, which resulted in a $2.41\,\%$ DER improvement on the CALLHOME dataset from the original paper [14]. In the history of diarization studies, it has been difficult to compare the results of pipeline approaches and EEND-based approaches because the former ones are often evaluated with an oracle speech activity detection (SAD), while EENDs operate SAD and diarization simultaneously. To conduct fair comparisons between pipeline and EEND-based approaches, this paper introduces SAD post-processing to align diarization results from EEND-EDA with external SAD results. We also propose an iterative inference for handling the problem of the number of outputs of EEND-EDA being empirically limited by its training dataset. We conduct thorough evaluations and analyses on simulated and real datasets including CALLHOME, CSJ, AMI, DIHARD II, and DIHARD III.

II. Related work

A. Speaker diarization

Conventional diarization methods are typically a pipeline of four modules: 1) speech activity detection (SAD), 2) speaker embedding extraction, 3) embedding clustering, and 4) overlap handling as an optional process. Most studies mainly focus on 2) speech embedding extraction and 3) embedding clustering. For speaker embeddings, i-vectors [18], [19], x-vectors [20]–[22], and d-vectors [6], [23]) have been explored. For embedding clustering, earlier works used traditional clustering algorithms *e.g.*, K-means clustering [24], [25], agglomerative hierarchical clustering (AHC) [8], [26], [27], mean-shift clustering [18], and spectral clustering [6], [28]. Recently, better clustering methods have been proposed such as variational Bayes hidden Markov model clustering (VBx) [29], [30], auto-tuning spectral clustering [7], or fully supervised clustering [23], [31]. They are usually used for hard clustering, so most pipeline methods (with some exceptions [32]) cannot deal with speaker overlap. To make them able to treat speaker overlap, 4) overlap handling should be considered; however, it has sometimes been excluded from methods and evaluations even in very recent studies [6], [7], [19], [23], [31]. Moreover, 1) speech activity detection has often been ignored in evaluations of pipeline approaches that use oracle speech activities [6], [7], [19], [23], [31].

Neural-network-based methods that directly produce diarization results from audio are emerging [9], [10]. One strength of such methods is that they require no extra modules for SAD or overlap handling. For some methods, models have been trained for speech separation, and diarization results have been obtained as byproducts [9], [10]. Such models have been trained on the basis of clean speech (or time-frequency masks calculated from clean speech); thus, they cannot be trained on real mixtures like DIHARD datasets [33], [34]. However, EEND-based models are trained to output multiple speakers' speech activities; they do not require clean speech for training and real mixtures can be used. The original EEND [11]–[13] can output diarization results for a fixed number of speakers. To extend the EEND for an unknown number of speakers, two approaches have been investigated. One is an attractor-based approach [14], and the other is a speaker-wise conditional EEND (SC-EEND) [15], [16]. In this paper, we investigate the attractor-based EEND because it showed better performance compared to SC-EEND.

B. Speech processing based on neural networks for unknown numbers of speakers

While some methods have achieved promising results with a fixed number of output speakers in diarization [11], [12], [35] and speech separation [36]–[39] contexts, it is challenging to make them able to deal with unknown numbers of speakers. The difficulty of neural-network-based speech processing for unknown numbers of speakers is that we cannot fix the output dimension.

One possible approach is to determine the maximum number of speakers to decode. In this case, the number of outputs is set to a sufficiently large value. Some methods treat a flexible number of speakers by outputting null speech activities if the number of outputs is smaller than the network capacity [40]. However, this approach did not work well with EEND (see [15]). In other methods, the number-of-speaker-wise output branches is trained independently, and the most probable is used during inference [41]. In this case, we have to know the maximum number of speakers. One of the strengths of EEND is that it can be finetuned using a target domain dataset from a pretrained model, but we usually cannot access the maximum number of speakers of the target domain beforehand. Therefore, a method that does not require that the maximum number of speakers be defined would be preferable.

Another approach is to decode speakers one by one until a stopping condition is satisfied, like SC-EEND [15]. For speech separation, RSAN [9], [10] and one-and-rest permutation invariant training (OR-PIT) [42] can be used. The key difference between speech separation and diarization is whether or not the residual output can be defined. RSAN uses a mask-based approach, in which each time-frequency bin is softly assigned to each speaker so that the process finishes when all the elements of the residual mask become zero. OR-PIT is time domain speech separation by which residual output is determined as a mixture that contains other speakers rather than the target speaker. Both require clean recordings to determine oracle masks or signals. However, they are not always accessible in the diarization context, in which only multi-talker recordings and speech segments are provided.

In this paper, we adopted an attractor-based approach like deep attractor networks (DANet) [40], [43]. While the number of speakers [43] or maximum number of speakers [40] is fixed for the original DANet, in this paper, we calculated a flexible number of attractors without defining them.

C. Neural-network-based representative vector calculation

There have several efforts made to calculate representatives from a sequence of embeddings in an end-to-end trainable fashion. For example, Set Transformer [44] enables set-to-set transformation, which can be used to calculate cluster centroids from a set of embeddings. However, the number of

outputs has to be known in advance, so it cannot be used for our purpose. Meier proposed an end-to-end clustering framework [45], in which clustering for all possible number of clusters $K \in \{1, \ldots, K_{\text{max}}\}$ is performed and the result of the most probable number of clusters is used. The framework performs the clustering of a flexible number of clusters in an end-to-end manner, but the maximum number of clusters is limited by K_{max}. EDA in this paper, in comparison, determines a flexible number of attractors from an input embedding without prior knowledge of the number of speakers.

III. Method

In this section, we first introduce the conventional EEND in Section III-A followed by an explanation of a natural extension of the method called attractor-based EEND in Section III-B. We also provide novel inference techniques in Section III-C.

A. Conventional end-to-end neural diarization

End-to-end neural diarization (EEND) [11], [12] is a method for estimating multiple speakers' speech activities simultaneously from an input recording. Given frame-wise F-dimensional acoustic features $(\boldsymbol{x}_t)_{t=1}^T$, where $t \in \{1, \ldots, T\}$ is a frame index, EEND estimates speech activities $(\boldsymbol{y}_t)_{t=1}^T$. Here, $\boldsymbol{y}_t \coloneqq [y_{1,t}, \ldots, y_{s,t}, \ldots, y_{S,t}]^\mathsf{T}$ denotes speech activities of S speakers at t defined as

$$y_{s,t} = \begin{cases} 0 & \text{(Speaker } s \text{ is inactive at } t) \\ 1 & \text{(Speaker } s \text{ is active at } t) \end{cases}. \tag{1}$$

EEND assumes that $y_{s,t}$ is conditionally independent given the acoustic features, namely,

$$P\left(\boldsymbol{y}_1, \ldots, \boldsymbol{y}_T \mid \boldsymbol{x}_1, \ldots, \boldsymbol{x}_T\right) = \prod_{t=1}^{T} \prod_{s=1}^{S} P\left(y_{s,t} \mid \boldsymbol{x}_1, \ldots, \boldsymbol{x}_T\right). \tag{2}$$

With this assumption, speaker diarization can be regarded as a multi-label classification problem and can thus be easily modeled using a neural network f_{EEND} as

$$(\boldsymbol{p}_1, \ldots, \boldsymbol{p}_T) = f_{\mathsf{EEND}}\left(\boldsymbol{x}_1, \ldots, \boldsymbol{x}_T\right), \tag{3}$$

where $\boldsymbol{p}_t \coloneqq [p_{1,t}, \ldots, p_{S,t}]^\mathsf{T} \in (0,1)^S$ is the posterior probabilities of S speakers' speech activities at frame index t. The estimation of speech activities $(\hat{\boldsymbol{y}}_t)_{t=1}^T$ is

$$\hat{\boldsymbol{y}}_1, \ldots, \hat{\boldsymbol{y}}_T = \underset{\boldsymbol{y}_1, \ldots, \boldsymbol{y}_T}{\arg\max}\, P\left(\boldsymbol{y}_1, \ldots, \boldsymbol{y}_T \mid \boldsymbol{x}_1, \ldots, \boldsymbol{x}_T\right), \tag{4}$$

$$= \left(\mathbb{1}\left(p_{s,t} > 0.5\right)\right)_{\substack{1 \le s \le S \\ 1 \le t \le T}}, \tag{5}$$

where $\mathbb{1}\left(\text{cond}\right)$ is an indicator function that returns 1 if cond is satisfied and 0 otherwise.

The conventional EEND is implemented as a composition of an embedding part $g : \mathbb{R}^{F \times T} \to \mathbb{R}^{D \times T}$ and a classification part $h : \mathbb{R}^{D \times T} \to (0,1)^{S \times T}$, *i.e.*,

$$f_{\mathsf{EEND}} = h \circ g. \tag{6}$$

The first embedding part g converts input acoustic features into D-dimensional frame-wise embeddings. It is implemented with N-stacked encoders, each of which converts a flexible length of embedding sequence $(\boldsymbol{e}_t^{(n-1)})_{t=1}^T$ into the same length of embedding sequence $(\boldsymbol{e}_t^{(n)})_{t=1}^T$ as

$$\boldsymbol{e}_1^{(n)}, \ldots, \boldsymbol{e}_T^{(n)} = g^{(n)}\left(\boldsymbol{e}_1^{(n-1)}, \ldots, \boldsymbol{e}_T^{(n-1)}\right), \tag{7}$$

$$\boldsymbol{e}_t^{(0)} = \boldsymbol{x}_t \quad (1 \le t \le T), \tag{8}$$

where $g^{(n)}$ is the n-th encoder layer. As examples of encoders, bi-directional long short-term memories (BLSTM) [11] and Transformers [12] are exploited in the conventional studies. In this paper, we used Transformer encoders but without positional encodings to prevent the outputs from being affected by the absolute position of the frames. Hereafter, for simplicity, we use $\boldsymbol{e}_t$ to denote the embeddings from the last encoder, *i.e.*, $\boldsymbol{e}_t \coloneqq \boldsymbol{e}_t^{(N)}$ for $t \in \{1, \ldots, T\}$.

Then, the classification part $h(\boldsymbol{e}; W_{\text{cls}}, \boldsymbol{b}_{\text{cls}})$ in (6) converts each embedding to posteriors of speech activities $(\boldsymbol{p}_t)_{t=1}^T$ in (3). It is implemented by using a fully connected layer and element-wise sigmoid function $\sigma(\cdot)$:

$$\boldsymbol{p}_t = \sigma\left(W_{\text{cls}}^\mathsf{T} \boldsymbol{e}_t + \boldsymbol{b}_{\text{cls}}\right) \in (0,1)^S, \tag{9}$$

where $(\cdot)^\mathsf{T}$ denotes the matrix transpose, and $W_{\text{cls}} \in \mathbb{R}^{D \times S}$ and $\boldsymbol{b}_{\text{cls}} \in \mathbb{R}^S$ are the weight and bias of the fully connected layer, respectively.

EEND outputs posteriors of multiple speakers simultaneously but without any conditions to decide the order of the speakers. Such a network is optimized by using a permutation-free objective [36], [46], which was originally proposed for multi-talker speech separation. It computes the loss for all possible speaker assignments between predictions $(\boldsymbol{p}_t)_{t=1}^T$, as introduced in (3), and groundtruth labels $(\boldsymbol{y}_t)_{t=1}^T$, and it picks the minimum one for backpropagation as follows.

$$\mathcal{L}_{\text{diar}} = \frac{1}{TS} \min_{(\phi_1, \ldots, \phi_S) \in \Phi(S)} \sum_{t=1}^{T} H\left(\boldsymbol{y}_t^\phi, \boldsymbol{p}_t\right), \tag{10}$$

where $\Phi(S)$ is a set of all possible permutations of the sequence $(1, \ldots, S)$, $\boldsymbol{y}_t^\phi \coloneqq [y_{\phi_1,t}, \ldots, y_{\phi_S,t}]^\mathsf{T} \in \{0,1\}^S$ is the permuted groundtruth labels, and $H(\cdot,\cdot)$ is the binary cross entropy defined as

$$H\left(\boldsymbol{y}_t, \boldsymbol{p}_t\right) \coloneqq \sum_{s=1}^{S} \left\{-y_{s,t} \log p_{s,t} - \left(1 - y_{s,t}\right) \log\left(1 - p_{s,t}\right)\right\}. \tag{11}$$

Compared with pipeline approaches, EEND has two significant strengths. One is that the pipeline approaches conduct diarization by dividing frame-wise speaker embeddings, so they require SAD as pre-processing and overlap detection and assignment as post-processing. In contrast, EEND estimates each speaker's speech activities independently, so no extra modules for speech activity detection and overlap detection are needed. The other strength is that the EEND model can be adapted to the desired domain's dataset, while pipeline approaches typically tune only probabilistic linear discriminant analysis (PLDA) parameters to optimize intra- and inter-speaker similarity between speaker embeddings [8], [17], [47].

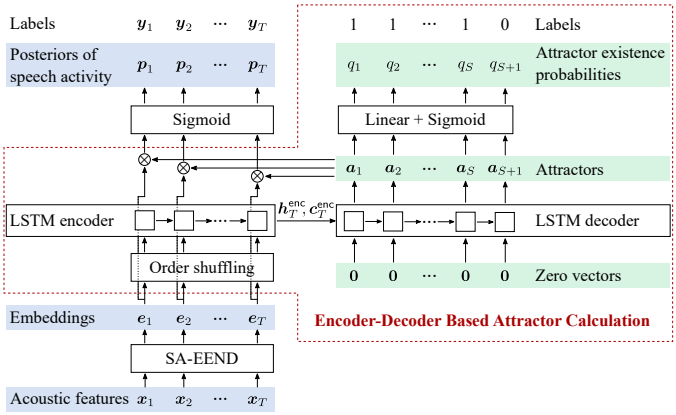

Fig. 1. EEND with encoder-decoder-based attractor calculation (EEND-EDA).

B. Attractor-based end-to-end neural diarization

The limitation of the conventional EEND is in the classification part h in (6); the number of output speakers S is fixed by the fully connected layer as in (9). One possible way to treat a flexible number of speakers with this fixed-output architecture is to set the number of outputs to be large enough. However, as discussed in Section II-B, it requires knowing the maximum number of speakers in advance, and it has been already verified that such a strategy results in poor performance (see [15]). It is also a problem that the calculation cost of the permutation-free loss increases if we set a large number of speakers to be output. Therefore, a significant research question is how to output diarization results for a flexible number of speakers.

In this paper, we extend the conventional EEND to handle a flexible number of speakers. We assume that the embedding part g in (6) is implemented in the same manner as the conventional EEND described in Section III-A. Given frame-wise D-dimensional embeddings $\{\boldsymbol{e}_t\}_{t=1}^{T}$, our goal is to produce posteriors for a flexible number of speakers in the classification part h. To achieve this goal, we propose a method to calculate a flexible number of speaker-wise attractors from embeddings and then calculate diarization results on the basis of attractors and embeddings. The proposed method is depicted in Figure 1.

1) EDA: Encoder-decoder-based attractor calculation: EDA converts frame-wise embeddings into speaker-wise attractors using a sequence-to-sequence method with an LSTM encoder-decoder. The LSTM encoder h^{enc} takes the frame-wise embeddings as input and updates its hidden state $\boldsymbol{h}_t^{\mathsf{enc}}$ and cell state $\boldsymbol{c}_t^{\mathsf{enc}}$ as

$$\boldsymbol{h}_t^{\mathsf{enc}}, \boldsymbol{c}_t^{\mathsf{enc}} = h^{\mathsf{enc}}\left(\boldsymbol{e}_t, \boldsymbol{h}_{t-1}^{\mathsf{enc}}, \boldsymbol{c}_{t-1}^{\mathsf{enc}}\right) \qquad (t = 1, \dots, T)\,. \quad (12)$$

The hidden and cell states of the encoder are initialized with zero vectors, *i.e.*, $\boldsymbol{h}_0^{\mathsf{enc}} = \boldsymbol{c}_0^{\mathsf{enc}} = \boldsymbol{0}$. The LSTM decoder h^{dec} estimates speaker-wise attractors as

$$\boldsymbol{h}_s^{\mathsf{dec}}, \boldsymbol{c}_s^{\mathsf{dec}} = h^{\mathsf{dec}}\left(\boldsymbol{0}, \boldsymbol{h}_{s-1}^{\mathsf{dec}}, \boldsymbol{c}_{s-1}^{\mathsf{dec}}\right) \qquad (s = 1, 2, \dots)\,. \quad (13)$$

We treat the hidden state at each step $\boldsymbol{h}_s^{\mathsf{dec}} =: \boldsymbol{a}_s \in (-1, 1)^D$ as speaker s's attractor, whose dimensionality D is the same as that of the frame-wise embeddings $\boldsymbol{e}_t$. The hidden and cell states of the decoder are initialized by the final hidden and cell states of the encoder as

$$\boldsymbol{h}_0^{\mathsf{dec}} = \boldsymbol{h}_T^{\mathsf{enc}}, \quad (14)$$

$$\boldsymbol{c}_0^{\mathsf{dec}} = \boldsymbol{c}_T^{\mathsf{enc}}, \quad (15)$$

which is shown as a right arrow from the LSTM encoder to the LSTM decoder in Figure 1. In general applications of a sequence-to-sequence method, *e.g.*, speech recognition or machine translation, the output is sentences, *i.e.*, a sequence of words, so the order of output is fixed. However, EDA cannot determine the order of output speakers in advance because this order is determined by minimizing cross entropy as in (10); thus, the well-known strategy of teacher forcing cannot be used. Furthermore, the s-th attractor can correspond to a speaker that has not yet been output and is not decided by the $(s-1)$-th attractors. To make this attractor calculation procedure fully order-free, we input a zero vector as input at each step as in (13). This is why we chose an LSTM-based encoder-decoder rather than Transformer encoder-decoder, which requires input queries rather than zero vectors.

Here, the input order to the EDA encoder affects the output attractors because EDA is based on a sequence-to-sequence method. To investigate the effect of the input order, we tried two types of input orders: chronological and shuffled orders. In the chronological order setting, embeddings are input in the order of frame indexes as in (12). In the shuffled order setting, we use the following instead of (12) :

$$\boldsymbol{h}_t^{\mathsf{enc}}, \boldsymbol{c}_t^{\mathsf{enc}} = h^{\mathsf{enc}}\left(\boldsymbol{e}_{\psi_t}, \boldsymbol{h}_{t-1}^{\mathsf{enc}}, \boldsymbol{c}_{t-1}^{\mathsf{enc}}\right) \qquad (t = 1, \dots, T)\,, \quad (16)$$

where $(\psi_1, \dots, \psi_T)$ is a randomly chosen permutation of $(1, \dots, T)$.

The diarization results $\boldsymbol{p}_t$ in (3) are calculated on the basis of the dot product of the frame-wise embeddings and speaker-wise attractors ($\otimes$ in Figure 1):

$$\boldsymbol{p}_t = \sigma\left(A^{\mathsf{T}}\boldsymbol{e}_t\right) \in (0, 1)^S\,, \quad (17)$$

where $A := [\boldsymbol{a}_1, \dots, \boldsymbol{a}_S]$ is a speaker-wise attractor. The posteriors are optimized by using (10) in the same manner as the conventional EEND. This posterior calculation no longer depends on the fully connected layer, which determines the output number of speakers as in (9); therefore, EDA-based diarization can vary the output number of speakers.

Comparing (9) and (17), the conventional EEND can also be regarded as using fixed attractors W_{cls} (with bias $\boldsymbol{b}_{\text{cls}}$). In comparison, EDA calculates attractors from an input sequence of embeddings, which makes attractors adaptive to the embeddings. This makes EEND-EDA more accurate even under the fixed-number-of-speakers condition (see Table III).

2) Attractor existence probability: As in (13), we can obtain an infinite number of attractors. To decide when to stop the attractor calculation, we calculate the attractor existence probabilities from the calculated attractors by using a fully connected layer followed by sigmoid activation:

$$q_s = \frac{1}{1 + \exp\left(-\boldsymbol{w}_{\text{exist}}^{\mathsf{T}}\boldsymbol{a}_s + b_{\text{exist}}\right)}, \quad (18)$$

where $\boldsymbol{w}_{\text{exist}} \in \mathbb{R}^D$ and $b_{\text{exist}} \in \mathbb{R}$ are trainable weights and bias parameters of the fully connected layer, respectively.

During training, we know the oracle number of speakers S, so the training objective of the attractor existence probabilities is based on the first $(S+1)$-th attractors using the binary cross entropy defined in (11):

$$\mathcal{L}_{\text{exist}} = \frac{1}{S+1} H\left(\boldsymbol{l}, \boldsymbol{q}\right), \tag{19}$$

where

$$\boldsymbol{l} \coloneqq [\underbrace{1, \ldots, 1}_{S}, 0]^{\mathsf{T}}, \tag{20}$$

$$\boldsymbol{q} \coloneqq [q_1, \ldots, q_{S+1}]^{\mathsf{T}}. \tag{21}$$

The total loss is defined as the weighted sum of $\mathcal{L}_{\text{diar}}$ in (10) and $\mathcal{L}_{\text{exist}}$ in (19) with the weighting parameter $\alpha \in \mathbb{R}_+$ as

$$\mathcal{L} = \mathcal{L}_{\text{diar}} + \alpha \mathcal{L}_{\text{exist}}. \tag{22}$$

In this paper, we use $\alpha = 1$. This multi-task loss aims to optimize frame- and speaker-wise posteriors with $\mathcal{L}_{\text{diar}}$ and attractor existence probabilities with $\mathcal{L}_{\text{exist}}$. However, we found that the optimization of $\mathcal{L}_{\text{exist}}$ inhibits the minimization of $\mathcal{L}_{\text{diar}}$ during the training of a model with a flexible number of speakers, which is more important for improving diarization accuracy. Therefore, we use $\mathcal{L}_{\text{exist}}$ to update only the fully connected layer parameterized by $\boldsymbol{w}_{\text{exist}}$ and b_{exist} in (18). This is performed by using the following instead of (18):

$$\check{\boldsymbol{a}}_s \leftarrow \mathsf{NoGrad}\left(\boldsymbol{a}_s\right), \tag{23}$$

$$q_s = \frac{1}{1 + \exp\left(-\boldsymbol{w}_{\text{exist}}^{\mathsf{T}} \check{\boldsymbol{a}}_s + b_{\text{exist}}\right)}, \tag{24}$$

where $\mathsf{NoGrad}\left(\cdot\right)$ denotes the operation for cutting a computational graph to disable back propagation to the preceding layers.

During inference, we cannot access the oracle number of speakers; thus, it is estimated using q_s in (18) as follows.

$$\hat{S} = \max\left\{s \mid s \in \mathcal{Z}_+ \wedge q_s \geq \tau\right\}, \tag{25}$$

where $\tau \in (0, 1)$ is a thresholding parameter, which is set to 0.5 in this paper. We then use the first $\hat{S}$ attractors to calculate posteriors as in (17).

C. Inference methodology

1) SAD post-processing: Diarization methods, especially pipeline ones, are sometimes evaluated with oracle speech segments. When evaluated in such a way, the comparison between pipeline methods and EEND-methods becomes hard mainly because EEND-based methods perform SAD and diarization simultaneously. One reason evaluations of pipeline approaches are mainly based on oracle speech segments is to consider speaker errors and SAD errors separately. It is reasonable to use oracle speech segments to focus on reducing speaker errors. However, such segments are not accessible in real scenarios, and the existence of SAD errors may worsen the clustering performance, which directly affects the diarization accuracy. Thus, we believe that SAD errors should also be considered in the context of pipeline methods. However, it is hard to say how accurate the SAD should be for a fair comparison between pipeline and EEND-based methods. Therefore, to align with the the pipeline methods, we introduce SAD post-processing for evaluating EEND. With this method, we can conduct a fair comparison between pipeline and EEND-based methods with the same SAD. Note that it can be used to improve the diarization performance when an accurate external SAD system is given.

Algorithm 1: SAD post-processing.

Input : $(\boldsymbol{p}_1, \ldots, \boldsymbol{p}_T) \in (0,1)^{S \times T}$ `// Frame-wise posteriors`
$(z_1, \ldots, z_T) \in \{0,1\}^T$ `// SAD results`
Output: $(\hat{\boldsymbol{y}}_1, \ldots, \hat{\boldsymbol{y}}_T) \in \{0,1\}^{S \times T}$ `// Speech activities`

1 Compute $\hat{\boldsymbol{y}}_1, \ldots, \hat{\boldsymbol{y}}_T$ using (5) `// Initial results`
2 **foreach** $t \in \{1, \ldots, T\}$ **do**
3 **if** $\|\hat{\boldsymbol{y}}_t\|_1 > 0 \wedge z_t = 0$ **then** `// Filter FA`
4   $\hat{\boldsymbol{y}}_t \leftarrow [0, \ldots, 0]^{\mathsf{T}}$
5 **else if** $\|\hat{\boldsymbol{y}}_t\|_1 = 0 \wedge z_t = 1$ **then** `// Recover MI`
6   $s^* \leftarrow \arg\max_{s \in 1, \ldots, S} \boldsymbol{p}_t$
7   $\hat{\boldsymbol{y}}_t \leftarrow [0, \ldots, 0, \underset{s^*}{1}, 0, \ldots, 0]^{\mathsf{T}} \in \{0,1\}^S$

The SAD post-processing algorithm is described in Algorithm 1. Here, we assume that we have SAD results $z_1, \ldots, z_T$ in addition to frame- and speaker-wise posteriors $\boldsymbol{p}_1, \ldots, \boldsymbol{p}_T$. We first estimate speech activities as usual by using (5) (line 1). However, this estimation is not always consistent with SAD results. Thus, we first filter false alarms (FA) by using SAD results. For each frame (line 2), if it is estimated that some speakers are active while the speech activity should be zero (line 3), we update the estimations with a zero vector (line 4). This procedure will always improve DER if $z_1, \ldots, z_T$ are the oracle speech activities. We also recover missed frames (MI) if no speaker is estimated as active while the speech activity is one (line 5). For each of such frames, we treat the speaker with the highest posterior as an active speaker (line 6–line 7). Including the oracle SAD as input will also improve the DER because missed-frame errors are replaced by correct estimation or at least speaker errors.

2) Iterative inference: Even if the model is trained to output a flexible number of speakers, the output number of speakers is empirically limited by the maximum number of speakers in a recording observed during pre-training (see Table VI). How to output the results of more than N speakers even if the model is trained on at most N-speaker mixtures is still an open question. In this paper, we propose an iterative inference method to produce results for more than N speakers by applying EEND decoding with iterative frame selection.

Preliminarily, we first reveal the characteristics of the EEND models that consist of stacked Transformer encoders and EDA. A Transformer encoder involves neither recurrence nor convolutional calculation, and we do not use positional encoding in this paper; thus, the embedding part g in (6) is an order-free transformation. EDA contains an LSTM encoder-decoder, but if the order of the input sequence is shuffled, we can

Algorithm 2: Iterative inference.

Input : $\boldsymbol{x}_1, \ldots, \boldsymbol{x}_T$ // Acoustic features
f_{EEND} // EEND model
$S_{\text{max}} \in \mathbb{N}$ // Max #Speakers that EEND can output
Output: $\hat{Y} \in \{0,1\}^{S \times T}$

1 $\mathcal{T} \leftarrow \{1, \ldots, T\}$ // Frame set
2 $n = 1$ // Iteration counter
3 **while** true **do**
4 Compute $\hat{Y}^{(n)}$ by (26), (27), and (5) // Decoding
5 Update $\mathcal{T}$ by (28) // Silence frame selection
6 **if** $S^{(n)} < S_{\text{max}} \vee |\mathcal{T}| = 0$ **then**
7 **break**
8 $n \leftarrow n + 1$
9 $\hat{Y} \leftarrow \begin{bmatrix} \hat{Y}^{(1)} \\ \vdots \\ \hat{Y}^{(n)} \end{bmatrix}$

say that EDA does not depend on the input order, so the EDA's classification part h in (6) is also an order-free function. Therefore, EEND-EDA does not depend on the order of the input features, which make it possible to process features that are not extracted at equal intervals along the time axis, as in EEND as post-processing [48]. The proposed iterative inference also utilizes this characteristic.

Algorithm 2 shows the algorithm for iterative inference, which calculates speech activities and selects silence frames $\mathcal{T} \subset \{1, \ldots, T\}$ iteratively. The frame set $\mathcal{T}$ is initialized by all of the frames (line 1), and the iteration counter n is initialized with one (line 2). At the n-th iteration, we conduct two processes: decoding and silence frame selection.

1) **Decoding**: Acoustic features $\boldsymbol{x}_t$ of the selected frames $\mathcal{T}$ are fed into EEND, and the posteriors $\boldsymbol{p}_t^{(n)} \in (0,1)^{S^{(n)}}$ are obtained as

$$\left(\boldsymbol{p}_t^{(n)}\right)_{t \in \mathcal{T}} \leftarrow f_{\mathsf{EEND}}\left((\boldsymbol{x}_t)_{t \in \mathcal{T}}\right), \tag{26}$$

where $S^{(n)} \in \{0, \ldots, S_{\text{max}}\}$ is the number of decoded speakers, which corresponds to the speech activity of the $((n-1)S_{\text{max}}+1)$-th to $((n-1)S_{\text{max}}+S^{(n)})$-th speakers. These activities at $t \in \mathcal{T}^c := \{1, \ldots, T\} \setminus \mathcal{T}$ are set to zero as

$$\boldsymbol{p}_t^{(n)} \leftarrow [\underbrace{0, \ldots, 0}_{S^{(n)}}]^{\mathsf{T}}. \tag{27}$$

With the posteriors, diarization results $\hat{Y}^{(n)} = \left(\hat{\boldsymbol{y}}_1^{(n)}, \ldots, \hat{\boldsymbol{y}}_T^{(n)}\right)$ are computed using (5).

2) **Silence frame selection**: Given the diarization results decoded at the n-th iteration, we update the frame set to contain the remaining silent frames as

$$\mathcal{T} \leftarrow \left\{ t \;\middle|\; t \in \mathcal{T}, \left\|\hat{\boldsymbol{y}}_t^{(n)}\right\|_1 = 0 \right\}. \tag{28}$$

If the number of output numbers of speakers $S^{(n)}$ is smaller than the maximum output of EEND S_{max}, it is assumed that all the speakers are decoded and the iterative process is finished (line 6–line 7). If the number of remaining frames $|\mathcal{T}|$ is zero, we also stop the process. Otherwise, we increment the iteration count (line 8) and go to the next iteration.

Algorithm 3: Iterative inference with DOVER-Lap (or iterative inference+).

Input : $\boldsymbol{x}_1, \ldots, \boldsymbol{x}_T$ // Acoustic features
f_{EEND} // EEND model
$S_{\text{max}} \in \mathbb{N}$ // Max #Speakers that EEND can output
Output: $\hat{Y} \in \{0,1\}^{S \times T}$

1 **for** $S_{\text{limit}} = 1$ **to** S_{max} **do**
2 $\mathcal{T} \leftarrow \{1, \ldots, T\}$ // Frame set
3 $n = 1$ // Iteration counter
4 **while** true **do**
5 Compute $\hat{Y}^{(n)}$ by (26), (27), (5) // Decoding
6 **if** $n = 1$ **then**
7 Limit the number of speakers in $\hat{Y}^{(n)}$ by (29)
8 Update $\mathcal{T}$ by (28) // Silence frame selection
9 **if** $S^{(n)} < S_{\text{max}} \vee |\mathcal{T}| = 0$ **then**
10 **break**
11 $n \leftarrow n + 1$
12 $\hat{Y}_{S_{\text{limit}}} \leftarrow \begin{bmatrix} \hat{Y}^{(1)} \\ \vdots \\ \hat{Y}^{(n)} \end{bmatrix}$
13 $\hat{Y} \leftarrow \text{DOVER-Lap}\left(\hat{Y}_1, \ldots, \hat{Y}_{S_{\text{max}}}\right)$

After the iterative process is finished, the final results $\hat{Y}$ are obtained by concatenating the results calculated at each iteration (line 9). With iterative inference, the number of speakers to be decoded is no longer limited by the training dataset.

3) Iterative inference with DOVER-Lap (or iterative inference+): Despite iterative inference being able to produce more than S_{max} speakers' speech activities, it has a potential problem in that the speech activities of two speakers decoded at different iterations never overlap. For example, the $(S_{\text{max}}+1)$-th speaker's speech activities never overlap with those of the first S_{max} speakers. This is because the frames in which the first S_{max} speakers are active will not be processed in the second iteration. To ease this problem, we introduce DOVER-Lap [49], which is the extension of DOVER [50]. Both of them are methods for combining multiple diarization results on the basis of majority voting, but unlike DOVER, DOVER-Lap take speaker overlap into account. We used a modified version of DOVER-Lap presented in [17], in which the speaker assignment strategy when multiple speakers were ranked equally was slightly different from the original DOVER-Lap [49].

The algorithm of iterative inference incorporated with DOVER-Lap is shown in Algorithm 3. In this paper, we refer to this inference as iterative inference+. The difference from the iterative inference in Algorithm 2 is that we limit the number of speakers to decode at the first iteration with $S_{\text{limit}} (\leq S_{\text{max}})$ (line 6–line 7). After the decoding step at the

first iteration using (26), (27), and (5), we choose at most the first S_{limit} speakers' speech activities from $\hat{Y}^{(1)} := (\hat{y}_{s,t})_{s,t}$ as

$$\hat{Y}^{(1)} \leftarrow (\hat{y}_{s,t})_{\substack{1 \leq s \leq \min\left(S^{(1)}, S_{\text{limit}}\right) \\ 1 \leq t \leq T}} . \tag{29}$$

The other procedures are the same as those in Algorithm 2, and finally, we obtain S_{limit}-wise diarization results $Y_{S_{\text{limit}}}$ (line 12).

In iterative inference+, S_{limit} is varied from 1 to S_{max} (line 1), which results in S_{max} diarization results for each recording. We then combine them by using DOVER-Lap to obtain the final result $\hat{Y}$ (line 13). With this procedure, the k-th speaker's speech activities can be overlapped with those of the $\max(1, (k - S_{\text{max}} + 1))$-th to $(k + S_{\text{max}} - 1)$-th speakers.

IV. Experiments

A. Datasets

1) Simulated datasets: To train the EEND-EDA model, we created simulated speech mixtures from single-speaker recordings of the following corpora.

- Switchboard-2 (Phase I & II & III)
- Switchboard Cellular (Part 1 & 2)
- NIST Speaker Recognition Evaluation (2004 & 2005 & 2006 & 2008)

Note that these corpora are compatible with the Kaldi CALLHOME x-vector recipe[1].

We used the following simulation protocol to create multi-talker mixtures from single-speaker recordings:

1) Select N speakers,
2) For each speaker, randomly sample speech segments and concatenate them with silences that are interlaid between speech segments,
3) Mix the created N long recordings and a noise signal with a randomly determined signal-to-noise ratio,
4) Convolve a room impulse response with the mixture.

The detailed algorithm for creating simulated mixtures can be found in [11]. In the second process, we assume that the occurrence of an utterance is a Poisson process, so the duration of the silence between speech segments follows the exponential distribution $\frac{1}{\beta}\exp\left(-\frac{x}{\beta}\right)$, where β is the mean value. β can be used to control the overlap ratio of the mixtures. To obtain a similar overlap ratio among various numbers of speakers, we varied β according to the number of speakers as summarized in Table I.

2) Real datasets: For real datasets, we employed five multi-talker datasets below.

- **CALLHOME** [51]: A dataset that consists of telephone conversations whose average duration is two minutes. We used the splits provided in the Kaldi x-vector recipe[1], which are denoted as Part 1 and Part 2, respectively. Two- and three-speaker subsets were used in the fixed-number-of-speakers evaluations, which are denoted as CALLHOME-2spk and CALLHOME-3spk.
- **CSJ** [52]: A dataset that consists of monologues and dialogues of Japanese speech. In this paper, we used the dialogue part of the dataset. The average duration of the recordings is about 13 minutes. Following [53], we used 54 dialogue recordings out of 58.
- **AMI headset mix** [1]: A meeting dataset that consists of 100 hours of multi-modal meeting recordings. Each meeting session is about 30 minutes. We used *headset mix* recordings, which were obtained by mixing the headset recordings of all the participants. We used the split and reference RTTMs provided in the VBx paper [30].
- **DIHARD II** [33]: A dataset used in the second DIHARD challenge. We used single-channel audio, which is used for tracks 1 and 2. The dataset consists of recordings from 11 domains (including telephone data) with an average duration of about 7 minutes.
- **DIHARD III** [34]: A dataset used in the third DIHARD challenge. It also consists of recordings from 11 domains (including telephone data) with an average duration of about 8 minutes. The test set has two evaluation conditions called *core* and *full*. The core set is a subset of the full set, in which the recordings are selected to balance the duration of each domain. In terms of the number of speakers, the full set contains more recordings of two speakers than the core set.

Their statistics are summarized in Table II. Note that the recordings in CSJ, AMI, DIHARD II, and DIHARD III were sampled at $16\,\text{kHz}$, so we downsampled them to $8\,\text{kHz}$ to be aligned with those of the simulated datasets. We also note that the recordings of the CSJ corpus are in stereo, so we mixed them to create monaural recordings.

TABLE I
DATASETS OF SIMULATED MIXTURES.

Dataset	Split	#Spk	#Mixtures	β	Overlap ratio (%)
Sim1spk	Train	1	100,000	2	0.0
	Test	1	100,000	2	0.0
Sim2spk	Train	2	100,000	2	34.1
	Test	2	500	2	34.4
	Test	2	500	3	27.3
	Test	2	500	5	19.1
Sim3spk	Train	3	100,000	5	34.2
	Test	3	500	5	34.7
	Test	3	500	7	27.4
	Test	3	500	11	19.2
Sim4spk	Train	4	100,000	9	31.5
	Test	4	500	9	32.0
Sim5spk	Train	5	100,000	13	30.3
	Test	5	500	13	30.7

B. Training

For the embedding part g in (6) of the proposed EEND-EDA, we used four-stacked Transformer encoders with four attention heads without positional encodings, each of which outputs 256-dimensional frame-wise embeddings. The inputs for the model were log-scaled Mel-filterbank-based features. We first extracted 23-dimensional log-scaled Mel-filterbanks with a frame length of $25\,\text{ms}$ and frame shift of $10\,\text{ms}$. Each of them was then concatenated with those of the preceding and following seven frames, followed by subsampling with

[1]https://github.com/kaldi-asr/kaldi/tree/master/egs/callhome_diarization/v2

TABLE II
DATASETS OF REAL RECORDINGS.

Dataset	Split	#Spk	#Mixtures	Overlap ratio (%)
CALLHOME-2spk [51]	Part 1	2	155	14.0
	Part 2	2	148	13.1
CSJ [52]	—	2	54	20.1
CALLHOME-3spk [51]	Part 1	3	61	19.6
	Part 2	3	74	17.0
CALLHOME [51]	Part 1	2–7	249	17.0
	Part 2	2–6	250	16.7
AMI headset mix [1]	Train	3–5	136	13.4
	Dev	4	18	14.1
	Test	3–4	16	14.6
DIHARD II [33]	Dev	1–10	192	9.8
	Test	1–9	194	8.9
DIHARD III [34]	Dev	1–10	254	10.7
	Test (Core)	1–9	184	8.8
	Test (Full)	1–9	259	9.2

a factor of 10. As a result, a $345\ (= 23 \times 15)$ dimensional acoustic feature was extracted for each $100\,\mathrm{ms}$. In the AMI and DIHARD datasets, speaker turns are segmented at a resolution of $10\,\mathrm{ms}$. We used a subsampling factor of 5 for these datasets during inference, which results in acoustic features extracted each $50\,\mathrm{ms}$.

In this paper, we evaluated EEND-EDA for both fixed-numbers-of-speakers and unknown-numbers-of-speakers conditions; thus, a model was trained for each purpose. For the fixed-number-of-speakers evaluation, the model was first trained on the Sim$k$spk training set for 100 epochs and evaluated on the Sim$k$spk test set. We also adapted the model to CALLHOME-$k$spk for another 100 epochs to evaluate the model on real recordings. We used $k \in \{2, 3\}$ in this paper. For the unknown-number-of-speakers evaluation, the model that was trained on Sim2spk was finetuned by using the concatenation of Sim{1,2,3,4}spk or Sim{1,2,3,4,5}spk for 50 epochs. The model was also adapted to each target dataset for another 500 epochs.

For network training using simulated mixtures, we used the Adam optimizer [54] with the Noam scheduler [55] with 100,000 warm-up steps. For adaptation, we also used the Adam optimizer but with a fixed learning rate of 1×10^{-5}. For efficient batch processing during training, we split each recording into 500 frames when using Sim$k$spk and 2000 frames when using the adaptation sets. The batch size for training was set to 64.

C. Evaluation

As an evaluation metric, we used diarization error rates (DERs) defined as

$$\mathrm{DER} = \frac{T_{\mathrm{MI}} + T_{\mathrm{FA}} + T_{\mathrm{CF}}}{T_{\mathrm{Speech}}}, \tag{30}$$

where T_{Speech}, T_{MI}, T_{FA}, and T_{CF} denote the duration of total speech, missed speech, false alarm speech, and speaker confusion, respectively. Following the prior works in [11], [56], we used $0.25\,\mathrm{sec}$ of collar tolerance at each speech boundary for the Sim$k$spk, CALLHOME, and CSJ evaluation.

TABLE III
DERS (%) FOR TWO-SPEAKER EVALUATIONS. $0.25\,\mathrm{s}$ OF COLLAR TOLERANCE WAS ALLOWED.

	Simulated			Real	
Method	$\beta = 2$	$\beta = 3$	$\beta = 5$	CALLHOME-2spk	CSJ
i-vector + AHC	33.74	30.93	25.96	12.10	27.99
x-vector (TDNN) + AHC	28.77	24.46	19.78	11.53	22.96
BLSTM-EEND [11]	12.28	14.36	19.69	26.03	39.33
SA-EEND [12]	4.56	4.50	3.85	9.54	20.48
EEND-EDA (Chronol.)	3.07	2.74	3.04	8.24	18.89
EEND-EDA (Shuffled)	**2.69**	**2.44**	**2.60**	**8.07**	**16.27**

For AMI, DIHARD II, and DIHARD III, we allowed no collar tolerance. We emphasize that speaker overlaps were NOT excluded from the evaluations.

We also report Jaccard error rates (JERs) in addition to DERs. To calculate JER, first, the optimal assignment between reference and system speakers is calculated. JER is the average score of each reference speaker defined as

$$\mathrm{JER} = \frac{1}{S_{\mathrm{ref}}} \sum_{s=1}^{S_{\mathrm{ref}}} \frac{T_{\mathrm{FA}}^{(s)} + T_{\mathrm{MI}}^{(s)}}{T_{\mathrm{Union}}^{(s)}}, \tag{31}$$

where S_{ref} is the number of reference speakers, and $T_{\mathrm{MI}}^{(s)}$ and $T_{\mathrm{FA}}^{(s)}$ are the duration of the missed and false alarm speech calculated between speech activities of the s-th reference speaker and the paired system speaker, respectively. $T_{\mathrm{Union}}^{(s)}$ is the time duration in which at least one of the s-th reference speakers of a paired system speaker is active.

V. RESULTS

A. Fixed numbers of speakers

1) Two-speaker experiment: First, we evaluated our method under the two-speaker condition. In this case, the model was first trained on Sim2spk and then adapted to CALLHOME-2spk Part 1. For the EEND-based methods, we used the model trained on Sim2spk to evaluate the simulated datasets and the one adapted to CALLHOME-2spk Part 1 to evaluate CALLHOME-2spk Part 2 and CSJ. For EEND-EDA, we used the first two output attractors for speech activity calculation.

Table III shows the results of the two-speaker evaluation. We observed that the proposed method with the shuffled order setting achieved the best DERs. Despite EEND-EDA begin designed to deal with flexible numbers of speakers, it outperformed the conventional EENDs, *i.e.*, BLSTM-EEND and SA-EEND, which output diarization results for fixed numbers of speakers. This is because the conventional EEND can be regarded as a fixed-attractor-based method, while EEND-EDA is an adaptive-attractor-based method as described in the last paragraph of Section III-B. This flexibility of attractors makes the proposed method more accurate even in fixed-number-of-speakers evaluations.

2) Three-speaker experiment: We also evaluated the method under the three-speaker condition. We first trained the model on Sim3spk and then adapted it to CALLHOME-3spk Part 1. We validated the performance on Sim3spk using the model trained on Sim3spk and that on CALLHOME-3spk Part 2 using the model adapted to CALLHOME-3spk

TABLE IV
DERs (%) FOR THREE-SPEAKER EVALUATIONS. 0.25 s OF COLLAR TOLERANCE WAS ALLOWED.

Method	Simulated			Real
	$\beta = 2$	$\beta = 3$	$\beta = 5$	CALLHOME-3spk
x-vector (TDNN) + AHC	31.78	26.06	19.55	19.01
SA-EEND [12]	8.69	7.64	6.92	14.00
EEND-EDA (Chronol.)	13.02	11.65	10.41	15.86
EEND-EDA (Shuffled)	**8.38**	**7.06**	**6.21**	**13.92**

Part 1. We used the first three attractors to evaluate EEND-EDA's performance. As shown in Table IV, EEND-EDA with sequence shuffling performed best on both simulated and real datasets.

3) Effect of input order: For a better understanding of EDA, we tried various types of sequences as inputs on the models, each of which was trained on chronologically ordered sequences and shuffled sequences. We evaluated matched and unmatched conditions of orders, and we also evaluated the effect of reducing the sequence length by subsampling or using the last $1/N$ part of the sequences. Table V shows the results on Sim2spk ($\beta = 2$). The EEND-EDA that was trained using chronologically ordered sequences performed well on chronologically ordered sequences but did poorly on shuffled sequences. It was also affected by subsampling, while it was slightly influenced by using the last $1/N$ part. These results indicate that the model that was trained on chronologically ordered sequences captured the tendency of speech length to decide output attractors. On the other hand, when the model was trained on shuffled sequences, it was not that affected by the order of sequences nor subsampling. However, when the last $1/N$ of the sequences were used, its performance degradation was worse than the model trained on chronologically ordered sequences. These results indicate that EDA trained on shuffled sequences captured the distribution of embeddings; thus, subsampling did not affect the performance that much, while using the last $1/N$, *i.e.*, biased sampling, degraded the DERs.

4) Embedding visualization: For intuitive understanding of the behavior of EDA, we visualized the embeddings $\boldsymbol{e}_t$ and attractors $\boldsymbol{a}_s$ within a two-speaker mixture from Sim2spk ($\beta = 2$) in Figure 2b. They were projected to two-dimensional space by using principal component analysis (PCA). We observed that the embeddings of two speakers were well distinguished from those of silence frames, and those of overlapped frames were distributed between the areas of the two speakers. For EEND-EDA, two attractors were calculated for each of the two speakers successfully as in Figure 2b. In Figure 2a, in comparison, the fixed attractors W_{cls} of the conventional EEND were not well separated compared with the attractors calculated using EDA.

To understand the characteristics of attractors from EDA, we also visualized the inter-mixture relationship of attractors. For visualization, we first chose an anchor speaker and then selected mixtures that contained the anchor speaker. We calculated two attractors from each mixture by using EEND-EDA and mapped them onto a two-dimensional space using PCA. The speaker assignment from the calculated attractors to speaker identifiers was based on the groundtruth labels. Figure 3 shows attractors of two-speaker mixtures that contain the same anchor speaker. It clearly shows that the each anchor speaker's attractors were not distributed near each other.

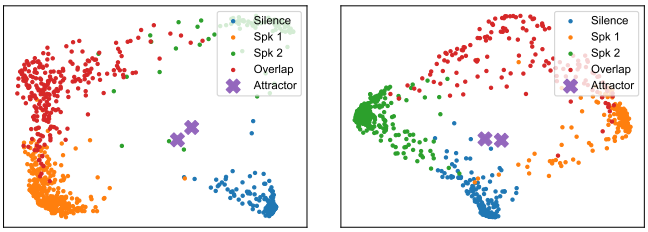

(a) Conventional EEND [12]

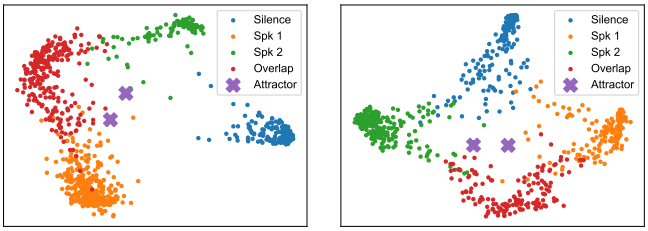

(b) EEND-EDA

Fig. 2. Visualization of embedding and attractors within each recording. For conventional EEND, weights of last fully connected layer W_{cls} were visualized instead of attractors.

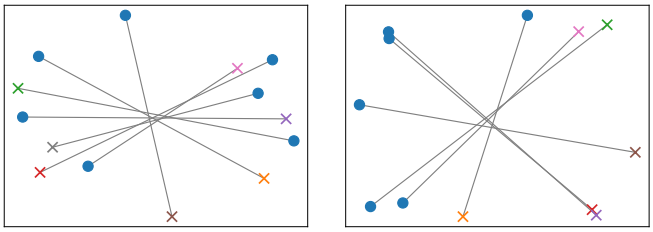

Fig. 3. Visualization of attractors across recordings. Selected speakers' attractors are marked by dots, and their interference speakers' attractors are marked by crosses. Colors of crosses correspond to speaker identities within each figure. Each pair of attractors from same mixture are connected with gray line.

From these results, the embeddings and attractors were calculated only to separate speakers in each mixture. We can also say that the attractors were not compatible with the speaker embeddings. This also supports the idea that attractors are adaptively calculated from input embeddings. A similar observation on attractors from DANet [43] in speech separation was provided in Section 5 of [57].

B. Unknown numbers of speakers

1) Simulated mixtures: To train EEND-EDA to output flexible numbers of speakers' results, we finetuned the model from the two-speaker model for at most 50 epochs using Sim1spk to Sim4spk or Sim1spk to Sim5spk. Table VI shows the step-by-step improvement of the model. Note that the results on the top row correspond to our previous paper [14]. First, disabling backpropagation from the attractor existence probabilities using (23) for EDA improved the DERs for

TABLE V
DERs FOR SIM2SPK ($\rho = 34.4\,\%$) USING VARIOUS TYPES OF SEQUENCES.

Method	Using whole sequence		Subsample $1/N$					Using the last $1/N$				
	Chronol.	Shuffled	$N=2$	$N=4$	$N=8$	$N=16$	$N=32$	$N=2$	$N=4$	$N=8$	$N=16$	$N=32$
EEND-EDA (Train: Chronol.)	3.07	30.04	3.54	7.32	14.48	21.13	27.18	3.67	4.97	5.40	6.11	7.68
EEND-EDA (Train: Shuffled)	2.69	2.69	2.70	2.68	2.79	3.09	5.08	3.36	5.92	7.46	8.59	10.65

TABLE VI
STEP-BY-STEP IMPROVEMENT ON SIMULATED DATASETS. FOR SIM2SPK AND SIM3SPK, WE USED $\beta = 2$ AND $\beta = 5$, RESPECTIVELY. IN q_s COLUMN, WE SHOW WHICH EQUATIONS WERE USED TO CALCULATE ATTRACTOR EXISTENCE PROBABILITIES DURING TRAINING. RESULTS ON TOP ROW CORRESPOND TO ORIGINAL SETTING [14].

Training data	#Epochs	q_s	Sim$k$spk				
			$k=1$	$k=2$	$k=3$	$k=4$	$k=5$
$k \in \{1,\ldots,4\}$	25	(18)	0.39	4.33	8.94	13.76	N/A
$k \in \{1,\ldots,4\}$	25	(23)(24)	0.25	4.06	7.68	10.12	23.08
$k \in \{1,\ldots,5\}$	25	(23)(24)	0.21	4.22	8.25	10.75	13.70
$k \in \{1,\ldots,5\}$	50	(23)(24)	0.36	3.65	7.70	9.97	11.95

Sim1spk to Sim4spk. However, we observed that the model still did not perform well on Sim5spk, which was not included in the training set. Adding Sim5spk to the training set solved the problem as shown in the third row, which shows DERs that improved for Sim5spk from $23.08\,\%$ to $13.70\,\%$. This indicates that EEND-EDA's number of output speakers was empirically limited by its training datasets, even though it does not limit the number of output speakers with its network architecture. Increasing the number of training epochs further improved the DERs as shown in the last row. Hereafter, we use the model of the last row ($k \in \{1,\ldots,5\}$, 50 epochs, using (23) and (24) during training).

2) CALLHOME: Since the CALLHOME dataset does not include an official dev/eval split, we used the split provided in the Kaldi recipe and performed cross-validation. For comparison with the prior work on EEND, we also report the results obtained for Part 2 of the dataset using the model adapted to Part 1. For SAD post-processing described in Section III-C1, we used the TDNN-based SAD provided in the Kaldi ASpIRE recipe[2] and oracle speech segments.

We show the number-of-speakers-wise results of cross-validation in Table VIIa. We also show the results for only evaluated single speaker regions in brackets. For this purpose, we chose up the most probable speakers from each time frame of the EEND-EDA results for fair comparison with x-vector-based methods. EEND-EDA outperformed the state-of-the-art x-vector-based methods in total DERs. One reason is that EEND-EDA can handle speaker overlap, but it showed a competitive DER ($5.29\,\%$) even when speaker overlaps were excluded from the evaluation. Considering the number of speakers in a mixture, EEND-EDA did especially better than the x-vector-based methods with VBx clustering when the number of speakers was small (#Speakers=2,3,4), while it was worse or on par when the number of speakers was large (#Speakers=5,6,7). One reason is that the pretraining was based on mixtures with at most five speakers, and another reason is that mixtures of a larger number of speakers are rare in the CALLHOME dataset. Table VIIb shows the results on CALLHOME Part2. It clearly shows that EEND-EDA outperformed the other EEND-based methods [15], [16] by over two percent of absolute DER.

Table VIII shows confusion matrices for the speaker counting of x-vector (TDNN) + AHC, x-vector (ResNet101) + AHC + VBx [30], SC-EEND [15], and EEND-EDA on CALLHOME Part 2. Our method achieved a higher speaker counting accuracy than the other methods by a large margin.

3) AMI headset mix: We next evaluated our method on the AMI headset mix, which has a different domain from the pretraining data (telephone conversation vs. meeting). We trained the model on the training set for 500 epochs and evaluated it on the dev and eval sets. The oracle speech segments were also used for SAD post-processing.

The results are shown in Table IX. EEND-EDA outperformed the x-vector-based methods on both the dev and eval sets with the oracle SAD. Note that the x-vector-based methods tuned the PLDA parameters on the dev set, so the superiority of EEND-EDA was smaller on the dev set than the eval set.

4) DIHARD II & DIHARD III: Finally, we evaluated our method on the DIHARD II and III datasets, which contain recordings from multiple domains. In this evaluation, we used iterative inference with and without DOVER-Lap, each of which are described in Section III-C2 and Section III-C3, respectively, to deal with large numbers of speakers. For SAD post-processing, we used oracle segments and the system used in the Hitachi-JHU submission to the DIHARD III challenge [17].

The results are shown in Tables X and XI. We can see that iterative inference with DOVER-Lap (iterative inference+) consistently improved DERs. Compared with the x-vector-based methods, EEND-EDA performed best on DIHARD III full, while the x-vector-based methods were better on DIHARD II and DIHARD III core.

We show the number-of-speakers-wise DERs and JERs on DIHARD III in Table XII. Our method performed better when the number of speakers was small and worse when the number of speakers was large. This is why EEND-EDA performed well on DIHARD III full and worse on DIHARD II and DIHARD III eval. We also observed that the proposed iterative inference+ improved performance, especially in terms of JERs on a large number of speaker cases, but it was still worse than the x-vector method. Handling a large number of speakers with EEND is left for future work.

[2]https://github.com/kaldi-asr/kaldi/tree/master/egs/aspire/s5

TABLE VII
DERs (%) of CALLHOME. 0.25 s of collar tolerance was allowed. TDNN-based x-vector results were obtained with Kaldi recipe. DERs of single-speaker regions are reported in brackets. AHC: agglomerative hierarchical clustering, VB: Variational Bayes resegmentation [29], VBx: Variational Bayes HMM clustering [30].

(a) Results of cross-validation.

Method	SAD	#Speakers 2	3	4	5	6	7	Total
EEND-EDA	-	8.18	15.05	16.54	27.29	31.40	37.23	14.81 (8.68)
X-vector (TDNN) + AHC	TDNN	14.66	18.42	20.46	31.40	32.62	46.43	19.48 (10.25)
X-vector (TDNN) + AHC + VB	TDNN	11.68	17.22	19.71	30.24	32.07	46.49	17.80 (8.29)
EEND-EDA	TDNN	**6.79**	**13.74**	**15.53**	**25.25**	**27.65**	**34.49**	**13.36** (**7.12**)
X-vector (TDNN) + AHC	Oracle	13.68	17.04	17.89	29.96	32.55	45.20	18.04 (8.54)
X-vector (TDNN) + AHC + VB	Oracle	10.94	15.85	17.40	29.23	33.97	42.69	16.57 (6.63)
X-vector (ResNet101) + AHC + VBx [30]	Oracle	9.83	15.23	14.29	**19.24**	**25.76**	36.25	14.21 (**4.42**)
EEND-EDA	Oracle	**5.50**	**12.17**	**12.86**	23.17	27.96	**34.08**	**11.72** (5.29)

(b) Results on CALLHOME Part 2.

Method	SAD	DER
SC-EEND [15]	-	15.75
SAD-OD-fiert SC-EEND [16]	-	15.32
EEND-EDA (From [14])	-	15.29
EEND-EDA	-	**12.88**
X-vector (TDNN) + AHC	TDNN	19.43
X-vector (TDNN) + AHC + VB	TDNN	17.61
EEND-EDA	TDNN	**13.84**
X-vector (TDNN) + AHC	Oracle	17.02
X-vector (TDNN) + AHC + VB	Oracle	15.57
X-vector (ResNet101) + AHC + VBx [30]	Oracle	13.33
EEND-EDA	Oracle	**10.46**

TABLE VIII
Confusion matrices for speaker counting on CALLHOME Part 2. X-vector-based results were obtained with oracle SAD, while EEND-based results were obtained without external SAD.

(a) X-vector (TDNN) + AHC (Accuracy=56.4 %)

Pred. #Speakers \ Ref. #Speakers	1	2	3	4	5	6
1	**0**	2	1	0	0	0
2	0	**87**	19	3	0	0
3	0	59	**51**	14	3	2
4	0	2	4	**3**	2	1
5	0	0	0	0	**0**	0
6	0	0	0	0	0	**0**

(b) X-vector (ResNet101) + AHC + VBx [30] (Accuracy=72.0 %)

Pred. #Speakers \ Ref. #Speakers	1	2	3	4	5	6
1	**0**	21	3	0	0	0
2	0	**122**	22	2	0	0
3	0	3	**44**	7	0	0
4	0	2	5	**10**	2	1
5	0	0	0	1	**3**	0
6	0	0	0	0	0	**1**
7	0	0	0	0	0	1

(c) SC-EEND [15] (Accuracy=76.4 %)

Pred. #Speakers \ Ref. #Speakers	1	2	3	4	5	6
1	**0**	1	0	0	0	0
2	0	**134**	20	4	0	0
3	0	13	**51**	10	4	2
4	0	0	3	**6**	1	1
5	0	0	0	0	**0**	0
6	0	0	0	0	0	**0**

(d) EEND-EDA (Accuracy=84.4 %)

Pred. #Speakers \ Ref. #Speakers	1	2	3	4	5	6
1	**0**	1	0	0	0	0
2	0	**142**	7	1	0	0
3	0	5	**54**	4	0	0
4	0	0	13	**14**	4	1
5	0	0	0	1	**1**	2
6	0	0	0	0	0	**0**

TABLE IX
DERs and JERs (%) for AMI headset mix. No collar tolerance was allowed.

Method	SAD	Dev DER	Dev JER	Eval DER	Eval JER
EEND-EDA	-	21.93	25.86	21.56	29.99
X-vector (ResNet101) + AHC	Oracle	19.61	23.90	21.43	25.50
X-vector (ResNet101) + AHC + VBx [30]	Oracle	16.33	**20.57**	18.99	**24.57**
EEND-EDA	Oracle	**15.69**	22.19	**15.80**	26.68

VI. Conclusion

In this paper, we proposed an end-to-end speaker diarization method for unknown numbers of speakers using encoder-decoder-based attractor calculation module called EEND-EDA. To conduct fair comparisons between EEND-based methods and pipeline methods under the same SAD condition, we introduced SAD post-processing for EEND-based methods. We also proposed iterative inference to cope with the problem of EEND-EDA's number of outputs being empirically limited by its training dataset. The proposed EEND-EDA performed well in both fixed-number-of-speakers and flexible-number-of-speakers evaluations.

Future work will include EEND-EDA for a large number of speakers. EEND-EDA does not limit the maximum number of speakers with its network architecture, but it is empirically limited by the training datasets as shown in Table VI. One reason is that EEND-EDA decides the number of speakers by using a neural network trained in a fully supervised manner. Introducing unsupervised clustering into the model may make the method free from this problem.

References

[1] J. Carletta, "Unleashing the killer corpus: experiences in creating the multi-everything AMI Meeting Corpus," *Language Resources and Evaluation*, vol. 41, no. 2, pp. 181–190, 2007.

[2] S. Watanabe, M. Mandel, J. Barker, E. Vincent, A. Arora, X. Chang, S. Khudanpur, V. Manohar, D. Povey, D. Raj, D. Snyder, A. S. Subramanian, J. Trmal, B. B. Yair, C. Boeddeker, Z. Ni, Y. Fujita, S. Horiguchi, N. Kanda, T. Yoshioka, and N. Ryant, "CHiME-6 Challenge: Tackling multispeaker speech recognition for unsegmented recordings," in *CHiME-6*, 2020.

[3] Z. Chen, T. Yoshioka, L. Lu, T. Zhou, Z. Meng, Y. Luo, J. Wu, X. Xiao, and J. Li, "Continuous speech separation: Dataset and analysis," in *ICASSP*, 2020, pp. 7284–7288.

[4] C. Boeddeker, J. Heitkaemper, J. Schmalenstoeer, L. Drude, J. Heymann, and R. Haeb-Umbach, "Front-end processing for the CHiME-5 dinner party scenario," in *CHiME-5*, 2018.

[5] M. Delcroix, K. Zmolikova, T. Ochiai, K. Kinoshita, and T. Nakatani, "Speaker activity driven neural speech extraction," in *ICASSP*, 2021.

[6] Q. Wang, C. Downey, L. Wan, P. Andrew Mansfield, and I. Lopez Moreno, "Speaker diarization with LSTM," in *ICASSP*, 2018, pp. 5239–5243.

[7] T. J. Park, K. J. Han, M. Kumar, and S. Narayanan, "Auto-tuning spectral clustering for speaker diarization using normalized maximum eigengap," *IEEE Signal Processing Letters*, vol. 27, pp. 381–385, 2020.

[8] G. Sell and D. Garcia-Romero, "Speaker diarization with PLDA i-vector scoring and unsupervised calibration," in *SLT*, 2014, pp. 413–417.

[9] K. Kinoshita, L. Drude, M. Delcroix, and T. Nakatani, "Listening to each speaker one by one with recurrent selective hearing networks," in *ICASSP*, 2018, pp. 5064–5068.

[10] T. von Neumann, K. Kinoshita, M. Delcroix, S. Araki, T. Nakatani, and R. Haeb-Umback, "All-neural online source separation, counting, and diarization for meeting analysis," in *ICASSP*, 2019, pp. 91–95.

TABLE X
DERs AND JERs FOR DIHARD II EVAL. NO COLLAR TOLERANCE WAS ALLOWED.

Method	SAD	DER	JER
EEND-EDA	-	29.57	51.50
EEND-EDA (Iterative inference)	-	29.41	49.61
EEND-EDA (Iterative inference+)	-	**28.52**	**49.77**
X-vector (TDNN) + AHC + VBx [47]	BUT [47]	**27.11**	**49.07**
EEND-EDA	BUT [47]	30.48	51.78
EEND-EDA (Iterative inference)	BUT [47]	29.80	49.99
EEND-EDA (Iterative inference+)	BUT [47]	29.09	50.45
DIHARD II baseline [33]	Oracle	28.81	50.12
X-vector (TDNN) + AHC + VBx [47]	Oracle	**18.21**	N/A
X-vector (ResNet101) + AHC [30]	Oracle	23.59	43.93
X-vector (ResNet101) + AHC + VBx [30]	Oracle	18.55	**43.91**
EEND-EDA	Oracle	20.54	46.92
EEND-EDA (Iterative inference)	Oracle	21.00	45.30
EEND-EDA (Iterative inference+)	Oracle	20.24	45.62

TABLE XI
DERs AND JERs FOR DIHARD III EVAL. NO COLLAR TOLERANCE WAS ALLOWED.

		Core		Full	
Method	SAD	DER	JER	DER	JER
EEND-EDA	-	25.94	47.76	21.55	41.15
EEND-EDA (Iterative inference)	-	25.76	45.35	21.40	39.09
EEND-EDA (Iterative inference+)	-	**24.77**	**45.18**	**20.69**	**39.07**
X-vector (TDNN) + AHC + VBx [17]	Hitachi-JHU [17]	**22.99**	42.44	21.48	38.73
X-vector (TDNN) + AHC + VBx + OVL [17]	Hitachi-JHU [17]	24.58	**42.02**	21.47	**37.83**
EEND-EDA	Hitachi-JHU [17]	23.96	46.82	20.03	40.31
EEND-EDA (Iterative inference)	Hitachi-JHU [17]	24.41	44.70	20.30	38.47
EEND-EDA (Iterative inference+)	Hitachi-JHU [17]	23.43	44.93	**19.53**	38.78
DIHARD III baseline [34]	Oracle	20.65	47.74	19.25	42.45
X-vector (TDNN) + AHC + VBx [17]	Oracle	**16.89**	38.49	15.83	34.27
X-vector (TDNN) + AHC + VBx + OVL [17]	Oracle	18.20	**38.42**	15.65	**33.71**
X-vector (ResNet152) + AHC + VBx [58]	Oracle	16.56	38.72	15.79	34.46
EEND-EDA	Oracle	18.38	43.69	14.91	36.93
EEND-EDA (Iterative inference)	Oracle	18.87	41.58	15.21	35.08
EEND-EDA (Iterative inference+)	Oracle	17.86	41.69	**14.42**	35.30

TABLE XII
BREAKDOWN RESULTS OF DIHARD III EVAL FOR EACH NUMBER OF SPEAKERS WITH ORACLE SPEECH SEGMENTS.

(a) DER (%)

	#Speakers								
Method	1	2	3	4	5	6	7	8	9
X-vector (TDNN) + AHC + VBx	**1.30**	11.43	16.76	**23.09**	**44.99**	**26.43**	**25.61**	**35.57**	**2.03**
EEND-EDA	2.80	7.52	15.79	25.63	47.66	31.73	35.47	38.19	18.73
EEND-EDA (Iterative inference+)	1.47	**6.98**	**15.55**	26.32	47.48	31.44	34.79	38.26	14.99

(b) JER (%)

	#Speakers								
Method	1	2	3	4	5	6	7	8	9
X-vector (TDNN) + AHC + VBx	**2.40**	16.99	44.68	**44.70**	**66.17**	**53.32**	**56.05**	**56.71**	**8.01**
EEND-EDA	3.37	11.77	**38.70**	48.37	67.40	64.85	67.77	69.00	57.60
EEND-EDA + iterative inference+	3.31	**11.34**	39.60	48.76	68.46	62.41	62.65	65.36	41.23

[11] Y. Fujita, N. Kanda, S. Horiguchi, K. Nagamatsu, and S. Watanabe, "End-to-end neural speaker diarization with permutation-free objectives," in *INTERSPEECH*, 2019, pp. 4300–4304.

[12] Y. Fujita, N. Kanda, S. Horiguchi, Y. Xue, K. Nagamatsu, and S. Watanabe, "End-to-end neural speaker diarization with self-attention," in *ASRU*, 2019, pp. 296–303.

[13] Y. Fujita, S. Watanabe, S. Horiguchi, Y. Xue, and K. Nagamatsu, "End-to-end neural diarization: Reformulating speaker diarization as simple multi-label classification," arXiv:2003.02966, 2020.

[14] S. Horiguchi, Y. Fujita, S. Wananabe, Y. Xue, and K. Nagamatsu, "End-to-end speaker diarization for an unknown number of speakers with encoder-decoder based attractors," in *INTERSPEECH*, 2020, pp. 269–273.

[15] Y. Fujita, S. Watanabe, S. Horiguchi, Y. Xue, J. Shi, and K. Nagamatsu, "Neural speaker diarization with speaker-wise chain rule," arXiv:2006.01796, 2020.

[16] Y. Takashima, Y. Fujita, S. Watanabe, S. Horiguchi, P. Garcia, and K. Nagamatsu, "End-to-end speaker diarization conditioned on speech activity and overlap detection," in *SLT*, 2021.

[17] S. Horiguchi, N. Yalta, P. Garcia, Y. Takashima, Y. Xue, D. Raj, Z. Huang, Y. Fujita, S. Watanabe, and S. Khudanpur, "The Hitachi-JHU DIHARD III system: Competitive end-to-end neural diarization and x-vector clustering systems combined by DOVER-Lap," in *DIHARD III*, 2021.

[18] M. Senoussaoui, P. Kenny, T. Stafylakis, and P. Dumouchel, "A study of the cosine distance-based mean shift for telephone speech diarization," *IEEE TASLP*, vol. 22, no. 1, pp. 217–227, 2014.

[19] G. Sell, D. Snyder, A. McCree, D. Garcia-Romero, J. Villalba, M. Maciejewski, V. Manohar, N. Dehak, D. Povey, S. Watanabe, and S. Khudanpur, "Diarization is hard: Some experiences and lessons learned for the JHU team in the inaugural DIHARD challenge," in *INTERSPEECH*, 2018, pp. 2808–2812.

[20] D. Snyder, D. Garcia-Romero, G. Sell, D. Povey, and S. Khudanpur, "X-vectors: Robust DNN embeddings for speaker recognition," in *ICASSP*, 2018, pp. 5329–5333.

[21] M. Diez, L. Burget, S. Wang, J. Rohdin, and J. Černockỳ, "Bayesian HMM based x-vector clustering for speaker diarization," in *INTERSPEECH*, 2019, pp. 346–350.

[22] X. Xiao, N. Kanda, Z. Chen, T. Zhou, T. Yoshioka, S. Chen, Y. Zhao, G. Liu, Y. Wu, J. Wu, S. Liu, J. Li, and Y. Gong, "Microsoft speaker diarization system for the VoxCeleb speaker recognition challenge 2020," in *ICASSP*, 2021.

[23] A. Zhang, Q. Wang, Z. Zhu, J. Paisley, and C. Wang, "Fully supervised speaker diarization," in *ICASSP*, 2019, pp. 6301–6305.

[24] S. H. Shum, N. Dehak, R. Dehak, and J. R. Glass, "Unsupervised methods for speaker diarization: An integrated and iterative approach," *IEEE TASLP*, vol. 21, no. 10, pp. 2015–2028, 2013.

[25] D. Dimitriadis and P. Fousek, "Developing on-line speaker diarization system," in *INTERSPEECH*, 2017, pp. 2739–2743.

[26] D. Garcia-Romero, D. Snyder, G. Sell, D. Povey, and A. McCree, "Speaker diarization using deep neural network embeddings," in *ICASSP*, 2017, pp. 4930–4934.

[27] M. Maciejewski, D. Snyder, V. Manohar, N. Dehak, and S. Khudanpur, "Characterizing performance of speaker diarization systems on far-field speech using standard methods," in *ICASSP*, 2018, pp. 5244–5248.

[28] D. Raj, Z. Huang, and S. Khudanpur, "Multi-class spectral clustering with overlaps for speaker diarization," in *SLT*, 2021, pp. 582–589.

[29] M. Diez, L. Burget, F. Landini, and J. Černocký, "Analysis of speaker diarization based on bayesian HMM with eigenvoice priors," *IEEE TASLP*, vol. 28, pp. 355–368, 2020.

[30] F. Landini, J. Profant, M. Diez, and L. Burget, "Bayesian HMM clustering of x-vector sequences (VBx) in speaker diarization: theory, implementation and analysis on standard tasks," arXiv:2012.14952, 2020.

[31] Q. Li, F. L. Kreyssig, C. Zhang, and P. C. Woodland, "Discriminative neural clustering for speaker diarisation," in *SLT*, 2021.

[32] Z. Huang, S. Watanabe, Y. Fujita, P. García, Y. Shao, D. Povey, and S. Khudanpur, "Speaker diarization with region proposal network," in *ICASSP*, 2020, pp. 6514–6518.

[33] N. Ryant, K. Church, C. Cieri, A. Cristia, J. Du, S. Ganapathy, and M. Liberman, "The Second DIHARD Diarization Challenge: Dataset, task, and baselines," in *INTERSPEECH*, 2019, pp. 978–982.

[34] N. Ryant, P. Singh, V. Krishnamohan, R. Varma, K. Church, C. Cieri, J. Du, S. Ganapathy, and M. Liberman, "The third DIHARD diarization challenge," arXiv:2012.01477, 2020.

[35] I. Medennikov, M. Korenevsky, T. Prisyach, Y. Khokhlov, M. Korenevskaya, I. Sorokin, T. Timofeeva, A. Mitrofanov, A. Andrusenko, I. Podluzhny, A. Laptev, and A. Romanenko, "Target-speaker voice activity detection: a novel approach for multi-speaker diarization in a dinner party scenario," in *INTERSPEECH*, 2020, pp. 274–278.

[36] D. Yu, M. Kolbæk, Z.-H. Tan, and J. Jensen, "Permutation invariant training of deep models for speaker-independent multi-talker speech separation," in *ICASSP*, 2017, pp. 241–245.

[37] Y. Luo, Z. Chen, J. R. Hershey, J. Le Roux, and N. Mesgarani, "Deep clustering and conventional networks for music separation: Stronger together," in *ICASSP*, 2017, pp. 61–65.

[38] Y. Luo and N. Mesgarani, "TasNet: time-domain audio separation network for real-time, single-channel speech separation," in *ICASSP*, 2018, pp. 696–700.

[39] ——, "Conv-TasNet: Surpassing ideal time–frequency magnitude masking for speech separation," *IEEE/ACM TASLP*, vol. 27, no. 8, pp. 1256–1266, 2019.

[40] Y. Luo, Z. Chen, and N. Mesgarani, "Speaker-independent speech separation with deep attractor network," *IEEE/ACM TASLP*, vol. 26, no. 4, pp. 787–796, 2018.

[41] N. Zeghidour and D. Grangier, "Wavesplit: End-to-end speech separation by speaker clustering," arXiv:2002.08933, 2020.

[42] N. Takahashi, S. Parthasaarathy, N. Goswami, and Y. Mitsufuji, "Recursive speech separation for unknown number of speakers," in *INTERSPEECH*, 2019, pp. 1348–1352.

[43] Z. Chen, Y. Luo, and N. Mesgarani, "Deep attractor network for single-microphone speaker separation," in *ICASSP*, 2017, pp. 246–250.

[44] J. Lee, Y. Lee, J. Kim, A. R. Kosiorek, S. Choi, and Y. W. Teh, "Set Transformer: A framework for attention-based permutation-invariant neural networks," in *ICML*, 2019, pp. 3744–3753.

[45] B. B. Meier, I. Elezi, M. Amirian, O. Dürr, and T. Stadelmann, "Learning neural models for end-to-end clustering," in *ANNPR*, 2018, pp. 126–138.

[46] J. R. Hershey, Z. Chen, J. Le Roux, and S. Watanabe, "Deep clustering: Discriminative embeddings for segmentation and separation," in *ICASSP*, 2016, pp. 31–35.

[47] F. Landini, S. Wang, M. Diez, L. Burget, P. Matějka, K. Žmolíková, L. Mošner, A. Silnova, O. Plchot, O. Novotný, H. Zeinali, and J. Rohdin, "BUT system for the Second DIHARD Speech Diarization Challenge," in *ICASSP*, 2020, pp. 6529–6533.

[48] S. Horiguchi, P. Garcia, Y. Fujita, S. Watanabe, and K. Nagamatsu, "End-to-end speaker diarization as post-processing," in *ICASSP*, 2021 (to appear).

[49] D. Raj, L. P. Garcia-Perera, Z. Huang, S. Watanabe, D. Povey, A. Stolcke, and S. Khudanpur, "DOVER-Lap: A method for combining overlap-aware diarization outputs," in *SLT*, 2021, pp. 881–888.

[50] A. Stolcke and T. Yoshioka, "DOVER: A method for combining diarization outputs," in *ASRU*, 2019, pp. 757–763.

[51] "2000 NIST Speaker Recognition Evaluation," https://catalog.ldc.upenn.edu/LDC2001S97.

[52] K. Maekawa, "Corpus of spontaneous Japanese: Its design and evaluation," in *ISCA & IEEE Workshop on Spontaneous Speech Processing and Recognition*, 2003.

[53] N. Kanda, C. Boeddeker, J. Heitkaemper, Y. Fujita, S. Horiguchi, K. Nagamatsu, and R. Haeb-Umbach, "Guided source separation meets a strong ASR backend: Hitachi/Paderborn University joint investigation for dinner party scenario," in *INTERSPEECH*, 2019, pp. 1248–1252.

[54] D. P. Kingma and J. Ba, "Adam: A method for stochastic optimization," in *ICLR*, 2015.

[55] A. Vaswani, N. Shazeer, N. Parmar, J. Uszkoreit, L. Jones, A. N. Gomez, L. u. Kaiser, and I. Polosukhin, "Attention is all you need," in *NeurIPS*, 2017, pp. 5998–6008.

[56] N. Kanda, S. Horiguchi, Y. Fujita, Y. Xue, K. Nagamatsu, and S. Watanabe, "Simultaneous speech recognition and speaker diarization for monaural dialogue recordings with target-speaker acoustic models," in *ASRU*, 2019, pp. 31–38.

[57] L. Drude, T. von Neumann, and R. Haeb-Umbach, "Deep attractor networks for speaker re-identification and blind source separation," in *ICASSP*, 2018, pp. 11–15.

[58] F. Landini, A. Lozano-Diez, L. Burget, M. Diez, A. Silnova, K. Žmolíková, O. Glembek, P. Matějka, T. Stafylakis, and N. Brümmer, "BUT system description for the Third DIHARD Speech Diarization Challenge," in *DIHARD III*, 2021.

PLACE PHOTO HERE

Shota Horiguchi Biography text here.

PLACE PHOTO HERE

Yusuke Fujita Biography text here.

PLACE PHOTO HERE

Shinji Watanabe Biography text here.

PLACE PHOTO HERE

Yawen Xue Biography text here.

PLACE PHOTO HERE

Paola García Biography text here.